# Hysteretic behavior of surface reactance of layered superconductor

S. S. Apostolov,[1,2] A. A. Bozhko,[2] Z. A. Maizelis,[1,2] M. A. Sorokina,[3] and V. A. Yampol'skii[1,2]

[1] *A.Ya. Usikov Institute for Radiophysics and Electronics, National Academy of Sciences of Ukraine, 61085 Kharkov, Ukraine*
[2] *V.N. Karazin Kharkov National University, 61077 Kharkov, Ukraine*
[3] *Aston University, Birmingham B4 7ET, UK*

We describe a nonlinear electromagnetic phenomenon in layered superconducting slabs irradiated from one side by an electromagnetic plane wave. We show that the surface reactance of the slab of the layered superconductor, as well as the reflectance of the incident wave, has the hysteretic behavior with jumps when changing the incident wave amplitude. This interesting nonlinear effect can be observed even at small amplitudes, when the wave frequency $\omega$ is close to the Josephson plasma frequency $\omega_J$.

PACS numbers: 74.78.Fk, 74.50.+r, 74.72.-h

## I. INTRODUCTION.

The unusual electrodynamic properties of layered superconductors (see, e.g., review Ref. 1 and references therein) attracted considerable attention due to their possible applications, including terahertz imaging, astronomy, spectroscopy, chemical and biological identification. A model in which the very thin superconducting $CuO_2$ layers are coupled by the intrinsic Josephson effect through the thicker dielectric layers was justified by the experiments for the **c**-axis conductivity in high-$T_c$ $Bi_2Sr_2CaCu_2O_{8+\delta}$ single crystals[1–5]. Within the model, a very specific type of plasma, the so-called Josephson plasma, is formed in layered superconductors. The current-carrying capability of this plasma is strongly anisotropic, not only in the absolute values of the current density. The physical nature of the currents along and across layers is quite different: the current along the layers is the same as in usual bulk superconductors, whereas the current across the layers originates from the Josephson effect. This Josephson current flowing along the **c**-axis couples with the electromagnetic field inside the insulating dielectric layers, causing a specific kind of elementary excitations called Josephson plasma waves (JPWs) (see, e.g., Ref. 1 and references therein). Therefore, the layered structure of superconductors favors the propagation of electromagnetic waves through the layers.

The electrodynamics of layered superconductors is described by nonlinear coupled sine-Gordon equations[1,6–10]. This nonlinearity originates from the nonlinear relation $J \propto \sin\varphi$ between the Josephson interlayer current $J$ and the gauge-invariant interlayer phase difference $\varphi$ of the order parameter. As a result of the nonlinearity, a number of nontrivial nonlinear phenomena[11–16] (such as slowing down of light, self-focusing effects, the pumping of weaker waves by stronger ones, etc.) have been predicted for layered superconductors. The nonlinearity plays a crucial role in the JPWs propagation, even for small wave amplitudes, $|\varphi| \ll 1$, when $\sin\varphi$ can be expanded into a series as $(\varphi - \varphi^3/6)$, for frequencies close to the Josephson plasma frequency. In Ref. 16 the transmittance of the layered superconducting slabs is studied. It is shown that the above mentioned nonlinearity leads to the sensitivity of the transmittance to the amplitude of the wave. This results in the hysteretic behavior of the transmittance when increasing/decreasing the amplitude. The similar nonlinear phenomena were observed in other media, e.g. in paramagnetic materials[17,18]. There the nonlinearity is originated from the nonlinear response of the media, described by Bloch equations.

In this paper, we continue our investigation of the nonlinear properties of superconducting slabs. Along with the decrease of the amplitude, the reflected wave experiences the phase shift $\alpha$. The latter is closely connected with the surface reactance $X$,

$$X = X_0 \tan\left(\frac{\alpha}{2}\right), \quad X_0 = \frac{4\pi}{c}\cos\theta, \tag{1}$$

where $\theta$ is the incident angle and $c$ is the light speed. The reactance and reflectivity of the slab are in focus in this paper. We describe an unusual strongly nonlinear phenomenon. The surface reactance of a superconducting slab being exposed to an incident wave from one of its sides depends not only on the wave frequency and the incident angle, but also on the wave amplitude. If the frequency $\omega$ of irradiation is close to the Josephson plasma frequency $\omega_J$, the reactance of the slab can vary over a wide range. This change is accompanied by the variation of the reflectance between the reflected and incident waves, from nearly one to zero. Moreover, the dependences of the reflectance and the surface reactance shows hysteretic behavior with jumps.

The large sensitivity of the problem parameters to the wave amplitude can be explained using a very clear physical consideration. Let us consider a wave frequency $\omega$ which is slightly smaller than the Josephson plasma frequency $\omega_J$. In this case, linear JPWs cannot propagate in the layered superconductor (see, e.g., Ref. 1). According to Refs. 11–13, the nonlinearity results in an effective decrease of the Josephson plasma frequency and, thus, nonlinear JPWs with high-enough amplitudes can propagate in the superconductor. So, the characteristics of the layered superconductor prove to be very sensitive to

the amplitude of the incident wave.

The paper is organized as follows. In section II, we formulate the problem and present the main equations for the electromagnetic fields both in the vacuum and in the slab of layered superconductor. In section III, we express the surface reactance $X$ and the reflectance $R$ of the slab in terms of the amplitude of the incident wave and analyze this dependence in two cases: when the frequency $\omega$ of the incident wave is either larger or smaller than the Josephson plasma frequency $\omega_J$. In both cases, we study the hysteretic features of these dependences. The results of numerical simulations support our theoretical predictions. In the last section we formulate a rather unexpected, but deep and useful analogy between the the propagation of the electromagnetic wave in the layered superconductor and the mechanical motion of a virtual particle in the central potential.

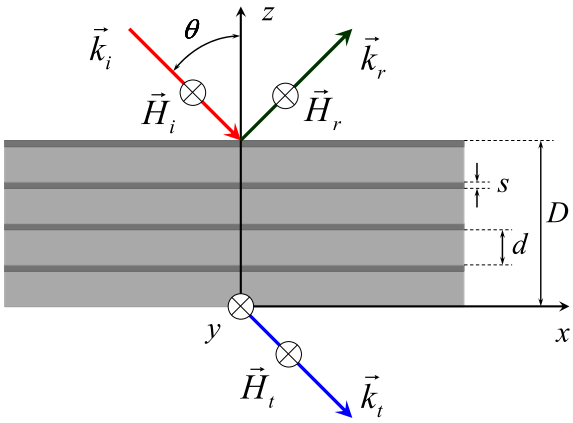


FIG. 1: (Color online) Geometry of the problem. A slab of layered superconductor is irradiated from the upper side by a $p$-polarized electromagnetic wave.

## II. SPATIAL DISTRIBUTION OF THE ELECTROMAGNETIC FIELD

### A. Geometry of the problem

We study a slab of layered superconductor of thickness $D$ (see Fig. 1). Superconducting layers of thickness $s$ are interlayed by insulators of much larger thickness $d$ ($s \ll d$). We assume the number of layers to be large, allowing the use of the continuum limit, and not considering the spatial distribution of the electromagnetic field inside each layer. The coordinate system is chosen in such a way that the crystallographic **ab**-plane coincides with the $xy$-plane, and the **c**-axis is along the $z$-axis. The plane $z = 0$ corresponds to the lower surface of the slab.

A monochromatic electromagnetic plane wave of frequency $\omega$ is incident on the upper surface of the slab, and it is partly reflected and partly transmitted through the slab. We consider the incident wave of the transverse magnetic polarization, with the magnetic field parallel to the surface of the slab,

$$\vec{E} = \{E_x, 0, E_z\}, \qquad \vec{H} = \{0, H, 0\}. \tag{2}$$

The incident angle $\theta$ is considered to be not close to zero, so that both non-zero components of the wave-vector $\vec{k}_i = \{k_x, 0, -k_z\}$ are of the order of $\omega/c$.

### B. Electromagnetic field in the vacuum

The magnetic field $H^+$ in the upper vacuum semispace ($z > D$) can be represented as a sum of the incident and reflected waves with amplitudes $H_i$ and $H_r$, respectively. The field $H^-$ in the vacuum semispace below the sample ($z < 0$) is the transmitted wave with amplitude $H_t$. The upper ($H^+$) and lower ($H^-$) fields and can be written in the following form,

$$H^+ = H_i \cos[k_x x - \omega t - k_z(z - D)] + H_r \cos[k_x x - \omega t + k_z(z - D) + \alpha], \tag{3}$$

$$H^- = H_t \cos(k_x x - \omega t - k_z z + \beta). \tag{4}$$

Here

$$k_x = \frac{\omega}{c}\sin\theta, \quad k_z = \frac{\omega}{c}\cos\theta, \tag{5}$$

are the components of the wave-vector $\vec{k}_i$ of the incident wave, $\alpha$ and $\beta$ are the phase shifts of the reflected and transmitted waves. Using Maxwell equations one can derive the electric field components in the vacuum:

$$E_x^+ = -H_i \cos\theta \cos[k_x x - \omega t - k_z(z - D)] + H_r \cos\theta \cos[k_x x - \omega t + k_z(z - D) + \alpha], \tag{6}$$

$$E_z^+ = -H_i \sin\theta \cos[k_x x - \omega t - k_z(z - D)] - H_r \sin\theta \cos[k_x x - \omega t + k_z(z - D) + \alpha], \tag{7}$$

$$E_x^- = -H_t \cos\theta \cos(k_x x - \omega t - k_z z + \beta), \tag{8}$$

$$E_z^- = -H_t \sin\theta \cos(k_x x - \omega t - k_z z + \beta). \tag{9}$$

### C. Electromagnetic field in the layered superconductor

The electromagnetic field inside a layered superconductor slab is determined by the distribution of the gauge-invariant phase difference $\varphi(x, z, t)$ of the order parameter between the layers (see, e.g., Ref. 1),

$$\frac{\partial H^s}{\partial x} = \frac{\mathcal{H}_0}{\lambda_c}\Big(\frac{1}{\omega_J^2}\frac{\partial^2\varphi}{\partial t^2} + \sin\varphi\Big), \tag{10}$$

$$E_x^s = -\frac{\lambda_{ab}^2}{c}\frac{\partial^2 H^s}{\partial z \partial t}, \qquad E_z^s = \frac{\mathcal{H}_0\lambda_c}{c}\frac{\partial\varphi}{\partial t}.$$

Here $\mathcal{H}_0 = \Phi_0/2\pi d\lambda_c$, $\Phi_0 = \pi c\hbar/e$ is the magnetic flux quantum, $\lambda_{ab}$ and $\lambda_c = c/\omega_J\epsilon^{1/2}$ are the London penetration depths across and along the layers, respectively. The Josephson plasma frequency is defined as

$$\omega_J = \sqrt{\frac{8\pi e d J_c}{\hbar\epsilon}}, \tag{11}$$

where $J_c$ is the critical value of the Josephson current density, $\epsilon$ is the permittivity of the dielectric layers in the slab. We omit the relaxation terms because, at low temperatures, they do not play an essential role in the phenomena considered here.

The phase difference $\varphi$ obeys a set of coupled sine-Gordon equations, that, in the continuous limit, takes on the following form (see, e.g., Ref. 1 and references therein):

$$\left(1 - \lambda_{ab}^2\frac{\partial^2}{\partial z^2}\right)\left[\frac{1}{\omega_J^2}\frac{\partial^2\varphi}{\partial t^2} + \sin\varphi\right] - \lambda_c^2\frac{\partial^2\varphi}{\partial x^2} = 0. \tag{12}$$

In this paper, we study the case of weak nonlinearity, when the Josephson current density $J_c\sin\varphi$ can be expanded as a series for small $\varphi$, up to the third order, $J_c\sin\varphi \approx J_c(\varphi - \varphi^3/6)$. We consider frequencies $\omega$ close to $\omega_J$ and introduce a dimensionless frequency,

$$\Omega = \frac{\omega}{\omega_J},$$

close to one. In this case, in spite of the weakness of the nonlinearity in Eq. (12), the *linear terms nearly cancel each other*, and the term $\varphi^3$ plays a crucial role in this problem. Moreover, when the frequency $\omega$ is close to the Josephson plasma frequency $\omega_J$, one can neglect the generation of higher harmonics[11,13].

It should be also noted that the nonlinearity provides an effective decrease of $\omega_J$. Indeed, the expression in the square brackets in Eq. (12) can be presented in the form $[(\omega_J^{\rm eff})^{-2}\partial^2\varphi/\partial t^2 + \varphi]$, where

$$\omega_J^{\rm eff} \approx \omega_J\Big(1 - \frac{\varphi^2}{12}\Big).$$

For not very small $\varphi$, the frequency of the incident wave can be greater than the effective Josephson plasma frequency $\omega_J^{\rm eff}$ and, therefore, the nonlinear Josephson plasma waves can propagate across the superconducting layers.

The $z$-component of the electric field induces a charge in the superconducting layers when the charge compressibility is finite. This results in an additional interlayer coupling (so-called, capacitive coupling). Such a coupling significantly affects the properties of the *longitudinal* Josephson plasma waves with wave-vectors perpendicular to the layers. The dispersion equation for linear Josephson plasma waves with arbitrary direction of the wave-vectors, taking into account capacitive coupling, was derived in Ref. 19. According to this dispersion equation, the capacitive coupling can be safely neglected in our case, when the wave-vector has a component $k_x \sim \omega/c$ along the layers, due to the smallness of the parameter $R_D^2\epsilon/sd$. Here $R_D$ is the Debye length for a charge in a superconductor.

We seek a solution of Eq. (12) in the form of a wave running along the $x$-axis,

$$\varphi(x,z,t) = a(z)|1-\Omega^2|^{1/2}\sin\big[k_x x - \omega t + \eta(z)\big], \tag{13}$$

with the $z$-dependent amplitude $a$ and phase $\eta$. We introduce the dimensionless $z$-coordinate,

$$\zeta = \frac{\kappa z}{\lambda_{ab}}, \quad \kappa = \frac{\lambda_c k_x}{|1-\Omega^2|^{1/2}}, \tag{14}$$

and the normalized thickness of the sample $\delta = D\kappa/\lambda_{ab}$.

Substituting the phase difference $\varphi$ given by Eq. (13) into Eq. (12), one obtains two differential equations for the functions $\eta(\zeta)$ and $a(\zeta)$. The first of them is

$$\eta'(\zeta) = \frac{L}{h^2(\zeta)} \tag{15}$$

where $L$ is an integration constant, prime denotes derivation over $\zeta$, and

$$h(\zeta) = \pm a(\zeta) - \frac{a^3(\zeta)}{8}. \tag{16}$$

The sign in this equation is plus for $\Omega < 1$ and minus for $\Omega > 1$, i.e., it is opposite to the sign of the following important parameter, the

$$\text{frequency detuning} = \Omega - 1.$$

The coupled sine-Gordon equations (12) give also the differential relation for $h(\zeta)$:

$$h'' = a + \frac{L^2}{h^3} + \frac{h}{\kappa^2}. \tag{17}$$

Equations (13), (15), (16), and (17) allow one to calculate the distribution of the phase difference $\varphi(x,z,t)$ and then, using Eq. (10), the electromagnetic field inside the superconducting slab.

## III. NONLINEAR RESPONSE OF THE SUPERCONDUCTING SLAB

### A. Main equations

In this section, we analyze the reflectance $R$ and the surface reactance $X$ of a slab of layered superconductor. We rewrite the expressions for the magnetic field $H^s$ and for the $x$-component $E_x^s$ of the electric field inside the slab using Eqs. (10) and Eq. (13),

$$H^s(x,\zeta,t) = -\mathcal{H}_0\frac{|1-\Omega^2|}{\kappa}h(\zeta)\cos(k_x x - \omega t + \eta(\zeta)\big), \tag{18}$$

$$E_x^s(x,\zeta,t) = \mathcal{H}_0\Gamma\frac{|1-\Omega^2|\cos\theta}{\kappa}\left[h(\zeta)\sin\big(k_x x - \omega t + \eta(\zeta)\big)\right]'.$$

Here we introduce the parameter

$$\Gamma = \frac{\lambda_{ab}\kappa}{\lambda_c\sqrt{\epsilon}\cos\theta},$$

which is small for the typical layered superconductors, $\Gamma \ll 1$. This is assumed throughout the paper.

Now we can find the unknown amplitudes of the reflected and transmitted waves by matching the magnetic fields and the $x$-components of the electric field at both interfaces (at $z = 0$ and $z = D$) between the vacuum and the layered-superconductor. Using Eqs. (18) for the fields in the superconductor and Eqs. (3), (4), (6), and (8) for the fields in the vacuum, we obtain the following three equations for the amplitudes $a(0)$, $a(\delta)$ and their derivatives on both surfaces of the layered superconductor:

$$\left(h(\delta) + \frac{\Gamma L}{h(\delta)}\right)^2 + \Gamma^2\left[h'(\delta)\right]^2 = 4h_i^2, \tag{19}$$

$$h^2(0) = \Gamma L, \tag{20}$$

$$a'(0) = 0. \tag{21}$$

Here

$$h_i = \frac{H_i}{\mathcal{H}_0}\frac{\kappa}{|1-\Omega^2|} \tag{22}$$

is the normalized amplitude of the incident wave. These three equations, together with the coupled sine-Gordon equations (17), determine the integration constant $L$ and the spatial distribution of the magnetic field $h(\zeta)$ inside the layered superconductor for each amplitude $h_i$ of the incident wave. It is important to note that the constant $L$ defines directly the reflectance $R$ of the superconducting slab. Indeed, according to Eq. (20), we have

$$R = 1 - \frac{h^2(0)}{h_i^2} = 1 - \frac{\Gamma}{h_i^2}L. \tag{23}$$

The reflectance $X$ can be calculated as follows,

$$X = X_0\frac{1-\sqrt{1-S^2}}{S}, \quad S = \frac{\Gamma h(\delta)h'(\delta)}{2\sqrt{R}h_i^2}. \tag{24}$$

The nonlinearity of Eq. (17) leads to the multivalued dependences of the surface reactance $X$ and the reflectance $R$ on the amplitude $h_i$ of the incident wave. In the following subsections, we analyze these unusual dependences, for both cases of negative ($\Omega < 1$) and positive ($\Omega > 1$) frequency detunings.

### B. Response of a superconducting slab for $\omega < \omega_J$

We start with the case when the frequency of the incident wave is smaller than the Josephson plasma frequency. In this frequency range, the linear Josephson plasma waves cannot propagate in layered superconductors. This corresponds to an exponentially small transmittance in the slab, due to the skin effect. However, the nonlinearity promotes the wave propagation because of the effective decrease of the Josephson plasma frequency.

Solving Eq. (17) with the boundary conditions (19), (20), and (21) one can find the constant $L$ and the values of $h$ and $h'$ on the upper interface of the slab and then calculate the reflectance $R$ and the reactance $X$ using Eqs. (23) and (24), respectively. Figure 2 demonstrates the numerically-calculated dependences of $X(h_i)/X_0$ and $R(h_i)$.

To analyze these dependences, we consider the spatial distribution of the gauge-invariant phase difference $\varphi$ of the order parameter and the phase trajectories $a'(a)$. We show these curves $a'(a)$ in Fig. 3. An increase of the spatial coordinate $\zeta$ [which is essentially $z$, as defined in Eq. (14)] from zero to $\delta$ corresponds to the moving along the phase trajectory $a'(a)$. The point $\zeta = 0$ (i.e., $z = 0$) corresponds to the starting point on the trajectory.

According to Eq. (21), all phase trajectories start from the points where $a'(\zeta = 0) = 0$. Different trajectories in $a'$ versus $a$ plane can be characterized by the values of $a(\zeta = 0) = a_0$ in these starting points. According to Eqs. (16) and (20), the value of $a_0$ defines the constant $L$ and, consequently, the whole trajectory determined by Eq. (17). Then, the value of the amplitude $h_i$ can be calculated from Eq. (19). So, dependences $X(h_i)$ and $R(h_i)$ are parametric with the parameter $a_0$.

The low-amplitude (quasi-linear) branch of the $R(h_i)$ dependence ranges within the interval $0 < h_i < (8/27)^{1/2}$ of the amplitudes of the incident waves. For small amplitudes $h_i \ll 1$, we deal with a linear problem, when the phase difference $\varphi$ and the electromagnetic field in the superconductor can be found in the form of linear combinations of exponential functions of $z$. In this case, the reactance $X$ and the reflectivity $R$ can be found asymptotically for sufficiently,

$$X(h_i \ll 1) = X_0\frac{\sqrt{1+4\tilde{\Gamma}^2\tanh^{-2}\tilde{\delta}}-1}{2\tilde{\Gamma}\tanh^{-1}\tilde{\delta}}, \tag{25}$$

$$R(h_i \ll 1) = \left(1+4\tilde{\Gamma}^2\sinh^{-2}\tilde{\delta}\right)^{-1},$$

Here $\tilde{\delta} = \delta\sqrt{1+\kappa^{-2}}$ and $\tilde{\Gamma} = \Gamma\sqrt{1+\kappa^{-2}}$. This reflectivity is very close to one regardless of the frequency detuning $(\Omega - 1)$. As we will see below, the "tanh" and "sinh" above, for $\omega < \omega_J$, will become "tan" and "sin" for $\omega > \omega_J$.

The phase trajectories that correspond to the low-amplitude solutions occupy the region $a < (8/3)^{1/2}$. For small $h_i$, these trajectories are close to the point $(a = 0, a' = 0)$ (as an example of such trajectory, see curve 5 in Fig. 3). An increase of the amplitude $h_i$ leads to the growth of the length of the phase trajectory and this length tends to $(a = \sqrt{8/3}, a' = \infty)$ when $h_i \to (8/27)^{1/2}$ (see curve 1 in Fig. 3).

The high-amplitude branches of the $X(h_i)$ dependence correspond to the solutions with $a(\zeta) > 8^{1/2}$. The high-

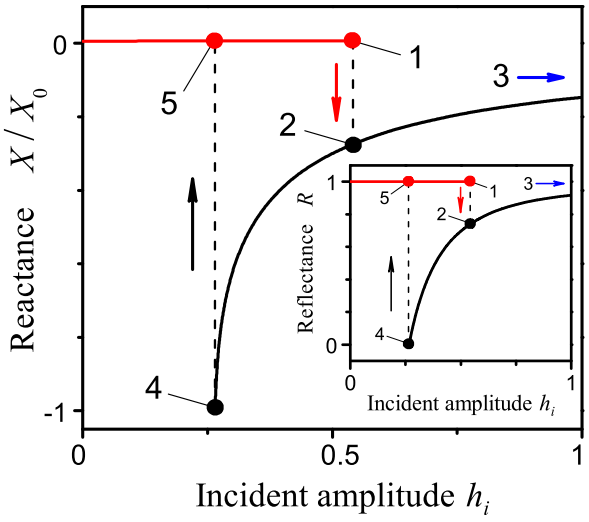


FIG. 2: (Color online) Dependences of the surface reactance $X$ [main panel], normalized on value $X_0$, and the reflectance $R$ [inset], on the normalized amplitude $h_i$ of the incident magnetic field, Eqs. (24), (1), (23) and (22), for different values of the *negative* frequency detuning: $(\Omega-1) = -4\cdot10^{-3}$. The vertical arrows show the hysteretic jumps when changing $h_i$. The numbers near the points on the curves correspond to the same numbers of the phase trajectories $a'(a)$ shown in Fig. 3. The values of the parameters are: $N = 200$, thickness of the slab is $D = 400$ Å, $\lambda_c = 4\cdot10^{-3}$ cm, $\lambda_{ab} = 2000$ Å, $\omega_J/2\pi = 0.3$ THz, and $\theta = 45°$.

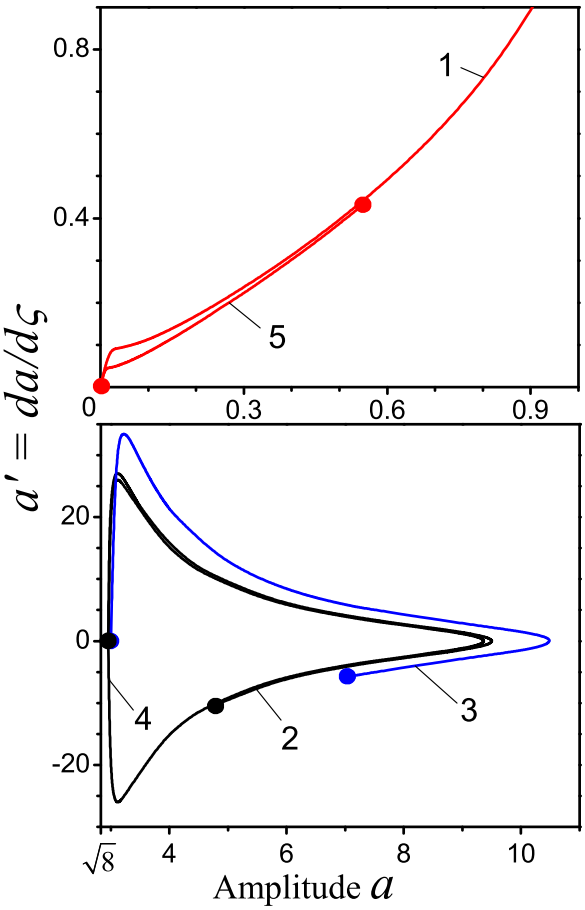


FIG. 3: (Color online) Phase trajectories $a'(a)$ for the *negative* frequency detuning $(\Omega - 1) = -4\cdot10^{-3}$. The numbers near the curves correspond to the same numbers near points in Fig. 2. Movement along the trajectories from the points with $a' = 0$ to the certain points, corresponds to the growth of the spatial coordinate $\zeta$ (proportional to $z$), from zero to $\delta$, inside the slab. The upper panel shows the region near the point $(a = 0, a' = 0)$. The bottom panel shows the region $a > \sqrt{8}$. The other parameters are the same as for Fig. 2.

amplitude solutions describe nonlinear Josephson plasma waves that can propagate in the layered superconductor even for negative frequency detuning (for $\Omega < 1$). The corresponding phase trajectories are closed curves (see the curve 4 in the lower panel in Fig. 3) or parts of the closed curves (e.g., curves 2 and 3). Note that the value of $h$ is negative for $a > 8^{1/2}$.

The oscillating character of the high-amplitude solutions results in smaller values of the reflectance, compared to the case of quasi-linear solutions. As seen in Fig. 2, the reflectance varies over a wide range, from nearly one to zero, depending on the amplitude $h_i$ of the incident magnetic field. It is important to note that the wavelengths of the nonlinear waves in the superconductor depend strongly on the incident wave amplitude $h_i$. So, changing $h_i$ one can control the relation between the wavelength and the thickness of the slab. The reflectance is very sensitive to this relation, and one can attain the complete absence of the reflected field by choosing the optimal value $h_{i,\min}$ of the amplitude $h_i$.

For high enough amplitudes $h_i$, the sample thickness $D$ is larger than the half-wavelength. In this case, the change of the coordinate $\zeta$ in the interval $0 < \zeta < \delta$ corresponds to the movement along a section of the phase trajectory loop (see the trajectories 2 and 3 in Fig. 3). When decreasing $h_i$, the wavelength increases, the movement along the phase trajectory approaches the complete loop, and the reflectance of the slab decreases. Finally, for a specific value of $h_i$, the wavelength becomes equal to the sample thickness, the phase trajectory draws a complete loop, the reflectivity becomes equal to zero (see the trajectory 4 in Fig. 3 and point 4 in Fig. 2). When $h_i$ is near $h_{i,\min}$ the reactance becomes close to $-X_0$.

In order to derive an analytical description of the high-amplitude branches we study two cases: $h_i \approx h_{i,\min}$ (and $R \ll 1$) and $h_i \gg 1$. In the first case the corresponding phase trajectories represent nearly complete loops. So, the amplitude dependence of the reflectance can be found asymptotically for not very thick slabs, $\delta \lesssim 1$, and presented in the following form,

$$R(h_i) = 1 - \left(\frac{h_{i,\min}}{h_i} + \frac{2\Gamma}{\delta}\sqrt{1 - \frac{h_{i,\min}^2}{h_i^2}}\right)^2. \qquad (26)$$

In the second case, when $h_i \gg 1$ or $a_0 \gg 1$, the asymptotical expression for reflectance is

$$R(h_i) = 1 - \frac{4\Gamma^2}{\delta^2}. \qquad (27)$$

It can be easily seen that the last asymptotics can be obtained from Eq. (26) by the formally substitution $h_i \to \infty$ in it. So, Eq. (26) can be treated as an interpolation formula for the whole high-amplitude branch of the $R(h_i)$ dependence.

In its turn, to describe the high-amplitude branch of the dependence $X(h_i)$ we return to the cases: $h_i \approx h_{i,\min}$ (and $R \ll 1$) and $h_i \gg 1$. In this two cases it can be write easily:

$$\frac{X(h_i)}{X_0} = \pm\frac{1-\sqrt{R(h_i)}}{\sqrt{1-R(h_i)}}. \qquad (28)$$

Here sign "+" is for $h_i \gg 1$ and sign "−" is for $h_i \approx h_{i,\min}$. In the intermediate region of $h_i$ the reactance changes the sign when the amplitude of the incident wave arrives at $\delta^2/\sqrt{2}$. So, for $\delta \gtrsim 1$ this value appears at the relatively great amplitudes and we can use Eq. (28) with sign "−" for almost whole high-amplitude branch of the $X(h_i)$ dependence.

In the case of the absence of the reflected wave ($R = 0$) both the electric and magnetic fields take on the same values on the upper and lower surfaces of the slab. Thus, the amplitudes of the incident and transmitted waves are equal. For not very thick slabs, $\delta \lesssim 1$, it happens for the amplitude $h_{i,\min} \simeq 2^{1/2}\Gamma\delta$. The corresponding spatial distribution of the magnetic field is shown by the solid curve in Fig. 4.

The nontrivial feature of $X(h_i)$ dependence can be seen from its hysteretic behavior with jumps. Let the amplitude $h_i$ of the incident wave increase from zero. In this case, the reactance is close to zero, and the $X(h_i)$ dependence follows the low-amplitude branch (see Fig. 2) and the reactance increases slowly near zero with $h_i$. When the amplitude reaches the critical value $(8/27)^{1/2}$ (point 1), further movement along this branch is impossible, and a jump to point 2, on the high-amplitude branch, occurs. A further increase in the amplitude $h_i$ results in a monotonic increase of the surface reactance $X$.

Afterwards, if the amplitude $h_i$ starts to decrease, then the $X(h_i)$ dependence does not follow the same track. Indeed, when the point 2 is passed, the reactance continues to follow the high-amplitude branch. Decreasing the amplitude $h_i$ results in a further decrease of the surface reactance. When $X$ becomes equal to $-X_0$ (point 5), it is not possible to continue the movement along the high-amplitude branch, and a return jump to the low-amplitude branch occurs. The analogous behavior is observed for the $R(h_i)$ dependence (see Fig. 2).

It should be noted that the jump from the low-amplitude branch (where the almost total reflection observed, $R \sim 1$) to the high-amplitude one (with smaller reflectivity) can be observed when changing the wave frequency $\omega$ for the constant amplitude $H_i$ of the incident wave. This jump occurs when the frequency detuning $(1-\Omega)$ becomes equal to the threshold value

$$(1-\Omega_{\rm cr}) = \frac{3}{4}\left(\lambda_c k_x \frac{H_i}{\mathcal{H}_0}\right)^{2/3}.$$

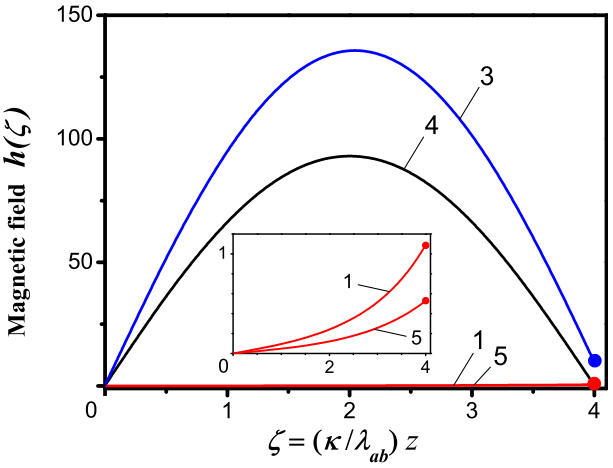


FIG. 4: (Color online) Spatial distribution of the amplitude $h$ of the magnetic field *inside* the superconducting plate. The numbers near the curves correspond to the same numbers near points in Fig. 2. Inset shows curves 5 and 1 on a large scale. Point 1 corresponds to the low-amplitude branch of the $R(h_i)$ and $X(h_i)$ dependences, when the reflection coefficient is close to one, and the reactance and the amplitude $h$ of the magnetic field near the lower interface ($z = 0$) of the slab are exponentially small. The reflectance $R$ for the point 4 is equal to zero, and the amplitudes of the fields near the upper and lower interfaces of the slab coincide. Here, the frequency detuning is $(\Omega - 1) = -5 \cdot 10^{-5}$, and the other parameters are the same as for Fig. 2.

### C. The reflective characteristic of a superconducting slab for $\omega > \omega_J$

Now we study the surface reactance and reflectivity of a layered superconducting slab for frequencies higher than the Josephson-plasma frequency, $\Omega > 1$. Contrary to the case $\Omega < 1$, even linear Josephson plasma waves can propagate in the layered superconductor. Therefore, the slab is not almost opaque and the reflectivity can vary over a wide range, depending on the relation between the wavelength and the thickness of the slab. Asimptotically we have

$$X(h_i \ll 1) = X_0 \frac{\sqrt{1+4\tilde{\Gamma}^2\tan^{-2}\tilde{\delta}}-1}{2\tilde{\Gamma}\tan^{-1}\tilde{\delta}}, \qquad (29)$$
$$R(h_i \ll 1) = \left(1+4\tilde{\Gamma}^2\sin^{-2}\tilde{\delta}\right)^{-1}.$$

Note that the "tanh" and "sinh" in Eq. (25), for $\omega < \omega_J$, has now been replaced by the "tan" and "sin" in Eq. (29), for $\omega > \omega_J$.

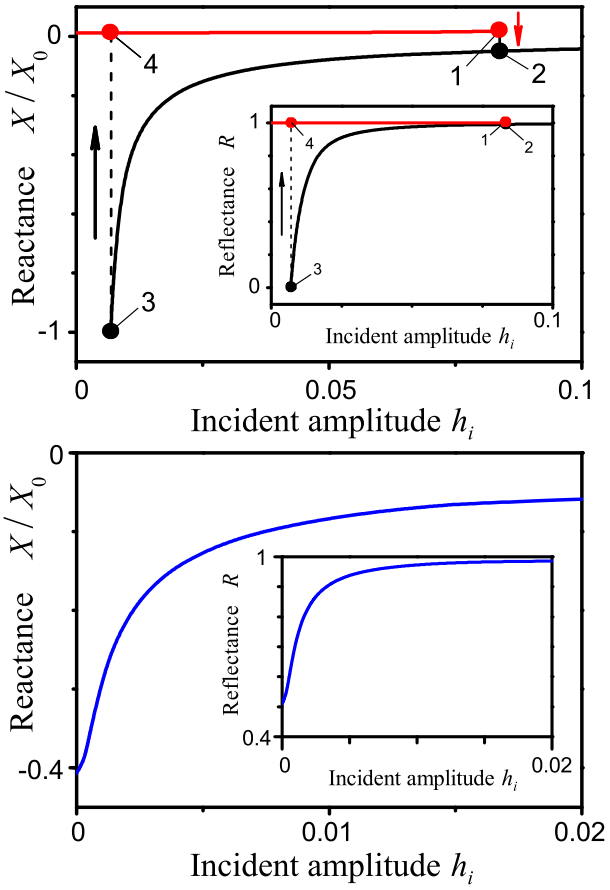


FIG. 5: (Color online) Dependence of the normalized reactance $X/X_0$ [main panels] and the reflectivity $R$ [insets] on the amplitude $h_i$ of the incident wave for different positive values of the frequency detuning: $\Omega-1=10^{-2}$, or $\tilde{\delta}/\pi=1.03$ (upper panel and inset); $\Omega-1=1.2\cdot10^{-2}$, or $\tilde{\delta}/\pi=0.94$ (lower panel and inset). Arrows show the change of the transmittance when changing $h_i$. The sample thickness is $D=4\cdot10^{-5}$ cm, and other parameters are the same as in Fig. 2.

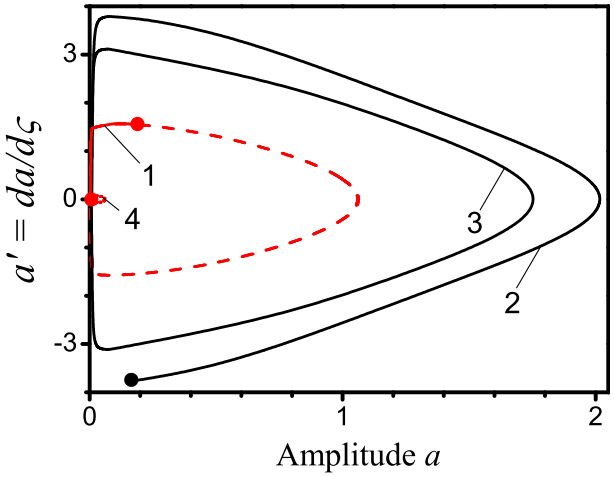


FIG. 6: (Color online) Phase trajectories $a'(a)$ for the *positive* frequency detuning $(\Omega-1)=10^{-2}$. The numbers near the curves correspond to the same numbers of points shown in the upper panel in Fig. 5. The solid lines show the portions of the phase trajectories that correspond to $0<\zeta<\delta$. The lower and upper surfaces of the slab correspond to the solid circles on the trajectories. The other parameters are the same as for Fig. 2.

In the nonlinear case, changing the amplitude $h_i$, one can control the relation between the wavelength of nonlinear wave and the thickness of the slab and, thus, the reflectivity is tunable by the amplitude of the incident wave. Figure 5 shows the $R(h_i)$ and $X(h_i)$ dependences for different positive frequency detunings.

The analysis based on Eqs. (16) (with choice of the sign "−"), (17), (19), (20), (21), (23) and (24) shows that the dependences $R(h_i)$ and $X(h_i)$ are reversible when the frequency detuning is larger than some threshold value. An example of such a reversible $R(h_i)$ dependence is presented by the dotted curve in Fig. 5.

The hysteresis in the $R(h_i)$ and $X(h_i)$ dependences appears for frequency smaller than the threshold value:

$$\omega<\omega_{\rm thr}\approx\omega_J+\left(\frac{D\sqrt{\epsilon}\sin\theta}{\sqrt{2}\pi\lambda_{ab}}\right)^2\omega_J. \qquad (30)$$

In this case, the reflectance can reach the zero value when the incident wave amplitude $h_i$ is first increased and then decreased. Namely, the incident wave amplitude $h_i$ is decreased after it is increased and a jump of $R(h_i)$ occurs from the low-amplitude branch to the high-amplitude one (see the solid curve and the inset in Fig. 5). One can derive the asymptotic equation for the optimal value $h_{i,\min}$ of $h_i$ when the superconducting slab becomes totally transparent ($R=0$),

$$h_{i,\min}\simeq\frac{3\sqrt{3}}{4I^2}\Gamma\delta^2, \qquad (31)$$

where

$$I=\int_0^1\frac{dx}{\sqrt{1-x^{4/3}}}=\frac{3}{4}\,\mathrm{B}\Big(\frac{1}{2},\frac{3}{4}\Big)\approx 1.7972$$

and $\mathrm{B}(x,y)$ is the Euler integral of the first kind.

It should be noted that the cause of the hysteresis for the positive frequency detuning differs from one for $\Omega<1$. This point is studied in more details in the next Section.

## IV. MECHANICAL ANALOGY

The problem discussed in this paper has a deep and very interesting mechanical analogy. Indeed, Eqs. (17) and (15) describe a motion of a virtual particle with unite mass in a centrally symmetric potential. In this analogy, the amplitude and phase [for $x=0$ and $t=0$] of the magnetic field, and the coordinate $\zeta$ across the layers of

the superconductor play the roles of the radial coordinate of the particle, its polar angle, and time, respectively. For example, accordingly to Eq. (10) for $0 < \zeta < \delta$ (in the slab) the radial coordinate is $-h(\zeta)$, the polar angle is $\eta(\zeta)$. Moreover, the constant $L$ in Eqs. (17) and Eq. (15) can be regarded as the conserved angular momentum of the particle for $0 < \zeta < \delta$.

Integrating Eq. (17) for the radial motion of the particle, we obtain the particle energy conservation law,

$$\frac{(h')^2}{2} + U_{\text{eff}}(h) = \mathcal{E}, \tag{32}$$

with the effective potential

$$U_{\text{eff}}(h) = \frac{L^2}{2h^2} + \frac{h^2}{2\kappa} - \int^h a(\tilde{h})\,\mathrm{d}\tilde{h}. \tag{33}$$

The first term in Eq. (32) describes the kinetic energy of the radial motion of the particle, $\mathcal{E}$ is the total energy of the particle. The first term in Eq. (33) is the centrifugal energy and the last two terms represent the potential of the central field.

The plot of the dependence $U_{\text{eff}}(h)$ is shown in Fig. 7 for the case of negative detuning ($\Omega < 1$). This dependence is three-valued and corresponds to the three branches of the function $a(h)$ (see Eq. (16)). Thus, the multivaluedness of the dependence $a(h)$ results in the multivaluedness of the effective potential $U_{\text{eff}}(h)$ and, therefore, there exist several possibilities for the particle motion. In terms of our electrodynamical problem, this means that several field distributions in the superconductor can be realized for the same amplitude $h_i$ of the incident wave.

Curve I in Fig. 7 shows the potential that corresponds to the low-amplitude solutions of our electrodynamical problem. The motion of the particle in this potential is monotonic that corresponds to the monotonic decrease of the field deep into the superconductor. According to Eq. (21), the stop-point (**???**) of the particle ($h' = 0$) corresponds to the lower boundary of the superconductor.

Since curve I is terminated in the point $h = (32/27)^{1/2}$, it cannot define the particle motion for high enough $h$. In this case, the particle moves in the potential described by curve II in Fig. 7. This motion is finite and periodical. It corresponds to the high-amplitude solutions of our electrodynamical problem. Curve III in Fig. 7 represents a branch of the $U_{\text{eff}}(h)$ dependence which cannot be realized when changing the amplitude $h_i$ of the incident wave.

Figure 8 shows a trajectory of the particle. This trajectory consists of three parts: the dotted circle with radius $h_t = h_i\sqrt{1-R}$ for $\zeta < 0$ (the lower vacuum semispace); the peculiar solid curve for $0 < \zeta < \delta$ (the layered superconducting slab); the dashed ellipse with semiaxes $h_i\sqrt{1+R}$ and $h_i\sqrt{1+R}\left(1-\sqrt{R}\right)^2/(1-R)$ for $\zeta > \delta$ (the upper vacuum semispace).

It is important to note that the trajectory is continuous, but it has turn points. Equations (19), (20), and (21)

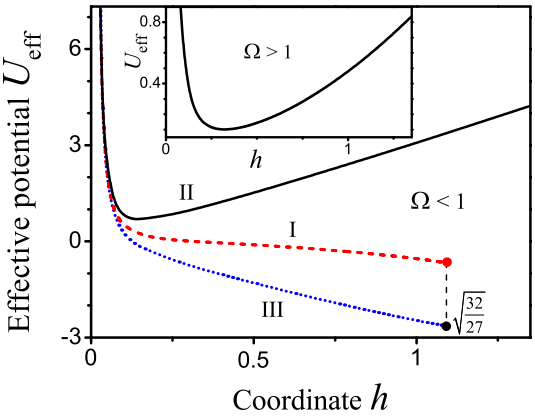


FIG. 7: (Color online) Dependence of the effective potential $U_{\text{eff}}$ defined by Eq. (33) on the radial coordinate $h$. The movement of the particle in this potential represents the mechanical analog for the spatial distribution of the amplitude $h$ of the magnetic field in the superconductor. The main panel shows curves I, II, and III that correspond to the three branches of the $a(h)$ dependence for the case of negative frequency detuning, $\Omega < 1$. The inset shows the $U_{\text{eff}}(h)$ curve for the opposite case, $\Omega > 1$, when only one branch of the $a(h)$ dependence exists. The value of constant $L$ is 0.1.

mean continuity of the magnetic field $H$, thus, the continuity of the particle coordinate. However, these equations do not imply the continuity of the particle velocity. Indeed, since the tangential component of the electrical field $E_x$, it can be calculated that on the surfaces of the layered superconducting slab ($\zeta = 0$ and $\zeta = \delta$) the direction of the velocity changes to opposite and its magnitude experiences a jump:

$$\frac{v(\zeta \to -0)}{v(\zeta \to +0)} = \frac{v(\zeta \to \delta + 0)}{v(\zeta \to \delta - 0)} = k_J k \lambda_{ab}^2, \tag{34}$$

where $k = \omega/c$ and $k_J = \omega_J/c$. As mentioned, the angular momentum is conserved for $0 < \zeta < \delta$ and equal to $L$. In the vacuum semispaces near the surfaces of the superconductor ($\zeta = 0$ and $\zeta = \delta$), it is equal to $-Lk_J k\lambda_{ab}^2$, so the angular momentum experiences jumps at $\zeta = 0$ and $\zeta = \delta$.

Now, we discuss the case of positive-frequency detuning. As seen in the inset in Fig. 7, the dependence of the potential $U_{\text{eff}}$ on the radial coordinate $h$ of the particle is single-valued. This is because the dependence $a(h)$ in Eq. (16) is single-valued in this case. Nevertheless, the dependence $X(h_i)$ can be multivalued even for $\Omega > 1$ (see Fig. 5). This feature seems to be paradoxical. Indeed, the particle motion is completely defined for any *initial conditions*. However, an assignment of the value of $h_i$ in relations (19), (20), and (21) does not mean an imposition of definite initial conditions for the particle motion. To illustrate this nontrivial feature of the electromagnetic wave transmission through a slab of layered superconductor, let us now consider the inverse problem. We wish to find the amplitude $h_i$ of the incident wave

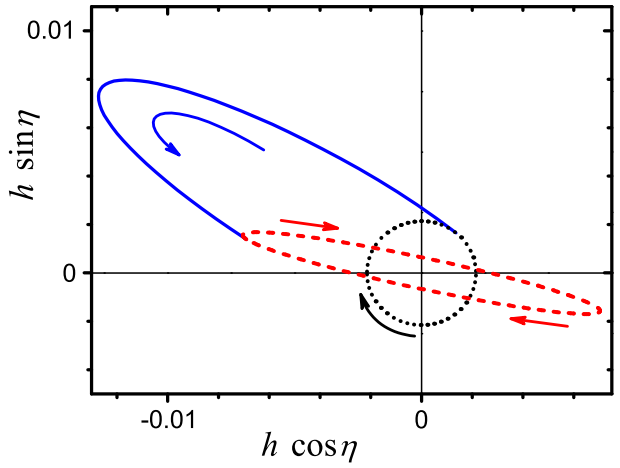


FIG. 8: (Color online) The trajectory of the virtual particle consisting of three parts, which correspond to three intervals of the time $\zeta$: the lower vacuum semispace, $\zeta < 0$ (dotted line); the layered superconducting slab, $0 < \zeta < \delta$ (solid line); the upper vacuum semispace, $\zeta > \delta$ (dashed line). Arrows shows the direction of the virtual particle motion when increasing the time $\zeta$. The negative frequency detuning $(\Omega - 1) = -2 \cdot 10^{-5}$, the normalized thickness $\delta = 0.18$, the incident amplitude $h_i = 0.004$, the reflectivity $R = 0.7$, $X = -0.22 X_0$ and other parameters are the same as in Fig. 2.

that is necessary to obtain a given value $h_t$ of the transmitted wave,

$$h_t = \frac{H_t}{\mathcal{H}_0} \frac{\kappa}{|1 - \Omega^2|}. \qquad (35)$$

According to Eq. (20), the value of $h_t$ defines unambiguously the angular momentum $L = h_t^2/\Gamma$ of the particle. On the basis of the motion equation (17) and the boundary condition Eq. (20) and (21), we can see that $h_t$ determines the trajectory in a single way. So, Eqs. (24) and (19) gives that the dependences $X(h_t)$ and $h_i(h_t)$ should be single-valued. However, this dependences is nonmonotonic if the condition Eq. (30) is satisfied. As a result, the dependence $X(h_i)$ appears to be multiple-valued.

## V. CONCLUSION

In this paper we describe a nonlinear phenomenon in layered superconductors. We show that the reflectivity $R$ and the surface reactance $X$ of a superconducting slab are sensitive to the amplitude of the incident wave due to the nonlinearity of the Josephson relation for the **c**-axis current. As a result, these quantities vary over a wide range [$R$ from near 1 to 0 and $X$ from 0 to $-X_0$, Eq. (1)], when changing the amplitude of the incident electromagnetic wave, and show the hysteretic behavior. It is important to note that, for frequencies close to the Josephson plasma frequency, this phenomenon can be observed even in the case of weak nonlinearity, when the interlayer phase difference $\varphi$ is small, $\varphi \ll 1$.

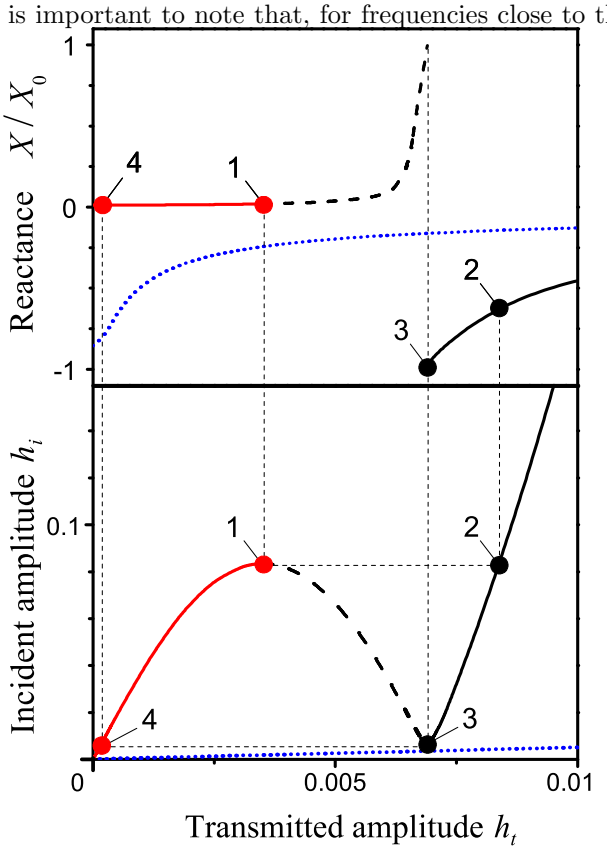


FIG. 9: (Color online) Solution of the inverse problem: dependences of the amplitude $h_i$ of the incident wave and the normalized reactance $X/X_0$ on the amplitude $h_t$ of the transmitted wave. The values of the parameters and the numbers near the indicated points are the same as in the main panel in Fig. 5. The dependences plotted by dotted curves are monotonic, leading to the single-valued dependence $X(h_i)$ (the lower panel in Fig. 5). The solid-and-dashed curves show the nonmonotonic behavior that results in the multivalued dependence $X(h_i)$ (the solid curve in the upper panel in Fig. 5).

## VI. ACKNOWLEDGEMENTS

[1] S. Savel'ev, V.A. Yampol'skii, A.L. Rakhmanov, and F. Nori, Rep. Prog. Phys. **73**, 026501 (2010).

[2] R. Kleiner, F. Steinmeyer, G. Kunkel, and P. Muller, Phys.

Rev. Lett. **68**, 2394 (1992).
[3] R. Kleiner and P. Muller, Phys. Rev. B **49**, 1327 (1994).
[4] E.H. Brandt, Rep. Prog. Phys. **58**, 1465 (1995).
[5] V.L. Pokrovsky, Phys. Rep. **288**, 325 (1997).
[6] S. Sakai, P. Bodin, and N.F. Pedersen, J. Appl. Phys **73**, 2411 (1993).
[7] S.N. Artemenko and S.V. Remizov, JETP Lett. **66**, 811 (1997).
[8] S.N. Artemenko and S.V. Remizov, Physica C **362**, 200 (2001).
[9] Ch. Helm, J. Keller, Ch. Peris, and A. Sergeev, Physica C **362**, 43 (2001).
[10] Yu.H. Kim and J. Pokharel, Physica C **384**, 425 (2003).
[11] S. Savel'ev, A.L. Rakhmanov, V.A. Yampol'skii, and F. Nori, Nat. Phys. **2**, 521 (2006).
[12] S. Savel'ev, V.A. Yampol'skii, A.L. Rakhmanov, and F. Nori, Phys. Rev. B **75**, 184503 (2007).
[13] V.A. Yampol'skii, S. Savel'ev, A.L. Rakhmanov, and F. Nori, Phys. Rev. B **78**, 024511 (2008).
[14] V.A. Yampol'skii, S. Savel'ev, T.M. Slipchenko, A.L. Rakhmanov, and F. Nori, Physica C **468**, 499 (2008).
[15] V.A. Yampol'skii, T.M. Slipchenko, Z.A. Mayzelis, D.V. Kadygrob, S.S. Apostolov, S.E. Savel'ev, and F. Nori, Phys. Rev. B **78**, 184504 (2008).
[16] S.S. Apostolov, Z.A. Mayzelis, M.A. Sorokina, V.A. Yampol'skii, and F. Nori, Phys. Rev. B **82**, 144521 (2010).
[17] A.A. Vertiy, S.P. Gavrilov, and S.I. Tarapov, Int. J. Infrared Millimeter Waves **13**, 9, 1403 (1992).
[18] A.A. Vertiy, S.P. Gavrilov, and S.I. Tarapov, Int. J. Infrared Millimeter Waves **14**, 3, 651 (1993).
[19] Ch. Helm and L.N. Bulaevskii, Phys. Rev. B **66**, 094514 (2002).